Virus Genes (2018) 54:199–214
https://doi.org/10.1007/s11262-017-1526-z

s8ORF2 protein of infectious salmon anaemia virus is a RNA-silencing suppressor and interacts with *Salmon salar* Mov10 (SsMov10) of the host RNAi machinery

Vandana Thukral[1] · Bhavna Varshney[1] · Rimatulhana B. Ramly[2] · Sanket S. Ponia[3] · Sumona Karjee Mishra[1,6] · Christel M. Olsen[2] · Akhil C. Banerjea[3] · Sunil K. Mukherjee[1] · Rana Zaidi[4] · Espen Rimstad[2] · Sunil K. Lal[1,5]

Received: 14 March 2017 / Accepted: 22 November 2017 / Published online: 7 December 2017

Abstract
The infectious salmon anaemia virus (ISAV) is a piscine virus, a member of *Orthomyxoviridae* family. It encodes at least 10 proteins from eight negative-strand RNA segments. Since ISAV belongs to the same virus family as Influenza A virus, with similarities in protein functions, they may hence be characterised by analogy. Like NS1 protein of Influenza A virus, s8ORF2 of ISAV is implicated in interferon antagonism and RNA-binding functions. In this study, we investigated the role of s8ORF2 in RNAi suppression in a well-established Agrobacterium transient suppression assay in stably silenced transgenic *Nicotiana xanthi*. In addition, s8ORF2 was identified as a novel interactor with SsMov10, a key molecule responsible for RISC assembly and maturation in the RNAi pathway. This study thus sheds light on a novel route undertaken by viral proteins in promoting viral growth, using the host RNAi machinery.

Keywords Viral suppressor of RNA silencing · Infectious Salmon Anaemia Virus · Segment 8 Open Reading Frame 2 · *Salmon salar* Mov10 · SsMov10

Introduction

Infectious salmon anaemia virus (ISAV) is a member of the *Orthomyxoviridae* family, and belongs to the genus *Isavirus* [1]. It is the causative agent of infectious salmon anaemia (ISA). Under normal conditions, ISA has only been detected in farmed Atlantic salmon (*Salmo salar*), and infected salmon exhibit clinical signs such as lethargy, anaemia, ascites, haemorrhagic liver, necrosis and congestion of internal organs [2]. The disease may result in high mortality with detrimental effects on farm production. Before the introduction of mandatory depopulation of net pens and production sites experiencing ISA outbreaks, the cumulative mortality during an outbreak could reach up to 90% [2–4].

The 14.3-kb genome of ISAV consists of eight single-stranded sense RNA segments, each ranging from 1.0 to 2.4 kb, encoding a total of 10 polypeptides [5–7]. The genomic segment 8 encodes two overlapping Open Reading Frames (ORFs) using a bicistronic coding strategy [8], similar to *Influenza A virus* segment 8, which encodes the non-structural (NS) protein. The smaller product of ISAV segment 8 ORF1 is 591 nucleotides long encoding a 22–24-kDa matrix protein, and the 726 nucleotides-long ORF2 encodes a 27.4-kDa protein (s8ORF2) [6, 9]. The s8ORF2 is a viral structural protein [8] having two nuclear localising signals (NLSs). It shows nuclear localisation early in the infection cycle and later on localises to the cytosol as well [8]. It binds RNA and antagonises cellular type I interferon (IFN) response [8]. A vertebrate host exhibits

Edited by Joachim Jakob Bugert.

✉ Sunil K. Lal
sunil.lal@monash.edu

1 Virology & Plant Molecular Biology Groups, International Center for Genetic Engineering and Biotechnology, Aruna Asaf Ali Road, New Delhi 110067, India

2 Norwegian University of Life Science, P.O. Box 8146 Dep., 0033 Oslo, Norway

3 Department of Virology, National Institute of Immunology, New Delhi 110067, India

4 Department of Biochemistry, Faculty of Science, Jamia Hamdard, New Delhi 110062, India

5 School of Science, Monash University, Sunway Campus, Selangor 47500, Malaysia

6 Prantae Solutions Pvt. Ltd., KIIT-Campus 11, Bhubaneswar, Odisha, India

two potent innate pathways for defence against viral infections: IFN and RNAi pathways [10–12]. In Atlantic salmon, ISAV-induced type I interferon response fails to restrict ISAV replication [13]. However, the potency of ISAV-responsive RNAi pathway in containing viral infection has not been studied so far.

In counter-defence to RNAi defence mechanism, viruses utilise their polypeptides to inhibit the innate RNAi pathway [14, 15]. The mechanism of action of these polypeptides is based on their binding to cellular factors like ds RNA, or interacting with other RNA-silencing factors, to inhibit the RNAi pathway [15, 16]. RNA viruses produce ds RNA, transiently, during replication, transcription etc. in the cytosol. The presence of ds RNA is a pre-requisite for triggering RNAi pathway. The host cell recognises ds RNA in the cell cytoplasm as a pathogen associated cellular marker [17] and initiates antiviral RNA-silencing mechanism in all eukaryotes [18–20]. During this process, viral ds RNA is processed by Dicer nuclease into 21–25 nucleotide long siRNA duplexes [18] which in turn are diverted to RNA-induced silencing complexes (RISC) to silence the target viral mRNA [19, 21–23]. Indeed, RNA viruses are known to be pre-emptive towards cellular defences and have adopted strategies to evade such cellular defence mechanisms (reviewed by [24] and [25]), by suppressing host RNAi pathways through a Viral Suppressor of RNAi or VSR [15, 26, 27]. A few of the VSRs of animal viral origin exhibit RNA binding and interferon antagonism simultaneously [28]. The VSR polypeptides, namely, Tat (HIV-1), NS1 (Influenza virus) and E3L (Vaccinia virus), VP35 (Ebolavirus) have three roles in common [29–32]. They all are interferon antagonists, secondly, they all bind to ds RNA molecules and thirdly, they interact with RNAi machinery components to block RNAi pathway.

In this study, we characterised s8ORF2 as a VSR of ISAV which interacts with SsMov10 in vitro. Among fish viruses; B2 protein of the fish Nodavirus, Striped Jack Nervous Necrosis Virus (SJNNV) as well as of Greasy Grouper Nervous Necrosis Virus (GGNNV) exhibit RNA-silencing suppressor activity by sequestering ds RNA [33–35]. This report identifies s8ORF2 as the third fish viral protein to be identified for RNAi suppressor function. It binds to ds RNA, siRNA and to *Salmo salar* Mov10 (SsMov10) of the RNAi pathway. Various domains were identified for RNAi suppression, RNA binding, SsMov10 interaction and dimerisation in vitro. The SsMov10 appears to play a significant role as s8ORF2 aide in RNAi suppression as it is a characterised RNA-induced Silencing Complex (or RISC—It is a multiprotein complex which uses miRNA or siRNA as the complementary strands and cleaves mRNA) maturing factor.

Materials and methods

Expression plasmids

Plant expression: the ISAV isolate Glesvaer/2/90 segment 8, ORF2 (s8ORF2) was PCR amplified (from pCR2.1-s8ORF2) and subcloned in pBI121 (Clontech) vector at *Xba*I/*Bam*HI sites.

Mammalian and piscine expressions: the s8ORF2 was cloned into pcDNA3.1 myc-His vector C (Invitrogen, Thermo-Fisher, Waltham, MA, USA) *Eco*RI/*Xho*I sites and its nonsense mutant NMs8ORF2 in *Eco*RI-*Xho*I sites. In NMs8ORF2, a G residue was added before the ATG by Phusion (Fermentas, Thermo-Fisher, Waltham, MA, USA). Cloning of SARS-7a, SARS- 3a and SARS-6a [36] and s8ORF2-EGFP [8] has previously been described. Cloning of SsMov10 was done in pcDNA at *Kpn*I4 and *Eco*RI sites.

Yeast Expression: Cloning of s8ORF2, ΔNTD, ΔCTD, ΔDD in *Eco*RI and *Bam*HI sites in both pGADT7 and pGBKT7 vectors. Cloning of SsMov10 was done in pGADT7 at *Nde*I and *Xho*I sites.

For bacterial expression, s8ORF2 was cloned in pGEX-4T-1 (Amersham, GE Healthcare) vector at *Eco*RI and *BamH*I sites. Deletion mutant s8ORF2$_{\Delta 1\text{-}61}$ (183 nt of the N-terminal) was PCR amplified and cloned in pGEX-4T-1 vector at *Eco*RI and *Bam*HI sites.

The bicistronic gene vector (RNAi-Ready-pSIREN-RetroQ-ZsGreen—abbreviated as Retro-Q; Clontech, CA, USA) transcribes the GFP under the CMV and the shGFP (small hairpin RNA against GFP) under the U6 promoters. Same vector with shGFP replaced with shLuc (unrelated shRNA control) was used for control experiments.

Agrobacterium-mediated tobacco transformation, plant materials, GFP imaging: reversal of silencing assay

All of the GFP-silenced T2 (second generation) tobacco plants lines showed red fluorescence under UV, indicating that the GFP transgene remained silenced in the T2 lines. The recombinant plasmids SARS-7a, SARS-6a, SARS-3a and s8ORF2 in pBI121 were transformed into *Agrobacterium tumefaciens*, LBA4404. The Agrobacterium culture was prepared in YEM (yeast extract mannitol) broth at 28 °C by incubation for 48 h, and harvested by centrifugation at 835 *g*. Two week old leaves of GFP-silenced transgenic lines grown under greenhouse condition [37] were used for the agroinfiltration mediated analysis.

The GFP fluorescence of leaves was monitored under UV (~ 302 nm) of UV transilluminator (HoeferTM

MacroVueUV-25, Amersham Biosciences). The leaves under UV were photographed by using digital cameras as described [37].

Dose-dependent FACS Analysis and GFP-reversal assay

The HEK293T cells were maintained in DMEM media with added Penicillin 100 µg/ml/Streptomycin 100 IU/ml, supplemented with 10% Foetal calf serum (FCS) and were transfected with 1.0 µg of RNAi ReadypSiren-RetroQ-ZsGreen-Retroviral vector using which Lipofectamine 2000 (Invitrogen, Thermo-Fisher, Waltham, MA, USA). SARS-7a and SARS-3a were used as positive controls and SARS- 6a was used as a negative control which were cotransfected in the control wells [36]. For dose-dependent analysis of wt-s8ORF2 and NMs8ORF2, increasing concentration of DNA from (100 to 500 ng) was cotransfected with the 1.0 µg of RNAi ReadypSiren-RetroQ-ZsGreen-Retroviral vector. The GFP expression was analysed 48 h post transfection. FACS was done in the BD–LSR system, and 60,000 cells were detected for each transfection. The results were analysed using WinMDI software.

Bacterial protein expression

BL21 *E. coli* cells were transformed with expression plasmids, and cultures were induced at 0.6 OD (600 nm) at 18 °C by 0.5 mM IPTG. Fusion proteins were affinity purified using Glutathione Sepharose 4B beads (GE Healthcare), and eluted in 20 mM glutathione and 50 mM Tris buffer (pH 8.0) using manufacturer's protocol.

Electromobility shift assay (EMSA)

Oligonucleotides: All the RNA and DNA oligonucleotides were obtained from Sigma. The sequence of the RNA oligonucleotides are, P1: 5′-GCAGCACGACUUCUUCAA GUC-3′ and the GO2: 5′-CUUGAAGAAGUCGUGCUG CUU-3′. The sequence of DNA oligonucleotides are U1: 5′ CGCTTGATGAGTCAGCCGGAA-3′ and L1: 5′ TTCCGG CTGACTCATCAAGCG-3′. GFP siRNA was generated by annealing P1 and GO2 oligonucleotides to a final concentration of 10 pmol/λ. DNA oligonucleotides L1 and U1 were annealed to obtain 10 pmol/λ of ds DNA oligo. 300-bp-long ss RNAs were generated from linearised M2-pCMV-tag2b (clone from our lab) plasmid using in vitro transcription kit (Ambion, Thermo-Fisher, Waltham, MA, USA). The plasmid was linearised either with *Sal*I or with *Hind*III, to transcribe from T3 to T7 promoter, respectively. Single-stranded RNAs thus obtained were annealed to obtain ds RNA, as mentioned above. The RNA was prepared from M2 of Influenza A virus in pCMV-tag-2b by transcription. The vector pCMV-tag-2b has T3 and T7 promoters in the opposite sides of MCS. Therefore, the M2 gene (291 bp) cloned in the MCS produces RNA molecules from forward (T3 promoter) and reverse (T7 promoter) directions. The products were DNase treated and quantified by spectroscopy. For ds RNA, the forward and reverse molecules synthesised were annealed before use for EMSA. *Labelling*: Kinasing of the siRNA was performed as per the manufacturers' instructions mentioned in T4-PNK kit (Fermentas, Thermo-Fisher, Waltham, MA, USA). Kinasing reaction was performed using GFP SiRNA (10 pmol) and [γ-^{33}P] ATP (60 µCi, Perkin-Elmer) in 15 µl reaction volume at 30 °C for 30 min. The reaction was stopped by adding 0.75 µl EDTA and incubating at 75 °C for 10 min.

EMSA: the assay was carried out as described [38]. Prior to sample loading, the 6% PAGE gel was pre-run at 80 V for 1 h and later on run in 1X TBE (45 mM Tris Borate, 1 mM EDTA) at 150 V, 4 °C. For competition experiments, unlabelled ss/ds RNA oligonucleotides, ss/ds DNA oligonucleotides, or ss/ds RNAs were used in 25 × and 50 × molar excess, in binding reaction prior to the addition of labelled siRNA (0.16 pmol). The protein–nucleic acid complexes were detected by autoradiography. For super-shift assay, the binding reaction was incubated with 1.0 µg of anti-s8ORF2 [8] or anti-His antibody (Santa-Cruz, USA) prior to the addition of labelled oligonucleotides.

Phage display, yeast two-hybrid assays

Purified GST-s8ORF2 polypeptide (1.0 ug) overlaid in microtitre plate for 16 h, while GST protein was used as a negative control. The bait protein was exposed to 12 mer Random peptide phage library (NEB, England), for 1 h, and supernatant with unreacting phages was discarded. Washing was performed thrice with 1X TBST. The eluted phages were titrated with ER2387. Then amplification, titrating, and sequence analysis was performed as per protocol.

The yeast two-hybrid assays were done by cloning the bait in pGADT7 and prey in pGBKT7 vectors and transfecting the DNA in AH109 yeast strain [39] as per manufacturer's protocol (Clontech, USA).

Immunostaining and microscopy

EPC cells (2×10^5 cells/well) transfected with pcDNA3.1 myc-His vector C-s8ORF2 and/or pcDNA-SsMov10-Flag construct were subjected to immunostaining 24 h post transfection. For the assay, cells were fixed in 80% acetone at 4 °C for 5 min followed by blocking in 5% skimmed milk. The cells were primary stained with] or anti-ISAV s8ORF2 antibody [8] and anti-flag (M2 Agilent 1:1000 in 3% foetal calf serum) followed by secondary staining with Alexa® Fluor 595-conjugated goat anti-rabbit IgG or 488-conjugated goat

anti-rabbit IgG (Molecular probes, Thermo-Fischer, USA). Non-saturated images were captured by a Plan-Apochromat 63/1.4 oil objective in a laser scanning confocal microscope (Zeiss Axiovert 200 M fluorescence, inverted microscope, equipped with a LSM 510 laser confocal unit and 488-nm argon laser, 546-nm helium/neon laser Z).

TCID50 calculation for virus titre determination

Virus solutions were quantified by measuring the tissue culture infective dose (TCID50 ml^{-1}) by end-point titration in 96-well culture plates. The cells were stained 5 d post inoculation using the ISAV-specific monoclonal antibody anti–NP (anti-ISAV, 1:500, Aquatic Diagnostics, Stirling, UK) with Alexa-488-labelled secondary antibody.

Western blot

Western Blot was performed to check for specificity of anti-ISAV antibodies, the transfection efficiency and status of infection. TO and EPC cells were transfected and infected as previously described; 0.5 ml ISAV (= $10^{6.25}$ $TCID_{50}$/25 µl) was used for TO cells. Cell lysates were prepared from infected and mock-infected cells 2 dpi, using RIPA buffer (50 mM Tris–HCl, pH 7.5, 150 mM NaCl, 2 mM EDTA, 1% Triton X-100). Aggregates and nuclei were removed by centrifugation (1150 *g*) for 5 min. Protein concentration was measured using Nanodrop. Samples were boiled in SDS sample buffer (Biorad) with reducing agent (Biorad). A total of 160.0 µg protein was loaded per well in precast 4–12% Bis–Tris polyacrylamide gels (Biorad) and separated by electrophoresis using XT-MOPS as running buffer (Biorad). After electroblotting onto a PVDF membrane (Biorad), the proteins were detected either with anti-ISAVs8ORF2 antiserum, anti-penta-his Mab or anti-ISAV antiserum (Aquatic Diagnostics, Stirling, UK) using HRP-conjugated secondary antibodies (GE healthcare) and ECL Plus Western Blotting Detection System (GE Healthcare, UK). The image was captured using Chemidoc XRS (Biorad).

Time dependence and dose dependence, real-time quantitative PCR Analysis

The TO cell line [40] originating from Atlantic salmon was used to propagate ISAV isolate Glesvaer/2/90 at 15 °C. The cell was seeded in six-well plates and maintained in Leibovitz's-15 (L-15, Gibco) medium supplemented with 2% foetal calf serum (FCS, PAA Laboratories), 2 mM L-glutamine, 0.04 mM β-mercaptoethanol and 0.05 mg/ml gentamycin-sulphate (Gibco) for propagation of cells. For inoculation of cells with ISAV, viral supernatant containing 1:10 dilution of $5 \times 10^{6.25}$ $TCID_{50}$/25 µl was used. Samples were collected at 0, 6, 24, 48 and 72 h post inoculation. In dose-dependence experiment, the ISAV supernatant containing 1:10 dilution of $10^{6.25}$ $TCID_{50}$/25 µl was serially diluted in 1:10 dilutions. The cells (TO) were infected with the (1) undiluted supernatant, and the following dilutions: (2) 1:10, (3) 1:100, (4) 1:1000, (5) 1:10 000, and results plotted in log scale.

Both total RNA isolations (RNeasy® Mini kit, Qiagen, Hilden, Germany) from ISAV-infected TO cells and cDNA synthesis (SuperScript IIIRT, Life Technologies, Carlsbad, California, USA) were performed according to the manufacturer's instructions. Elongation factor 1 alpha (EF1α) was used as a reference gene in RT-qPCR to normalise the Ct values [41, 42], sequences of which are given in Table 1. Reactions were carried out in 25 µl volumes containing master mix, 3 µl cDNA, and 300 nM of each primer targeting the EF1α, ISAV-segment 8 and Atlantic salmon Mov-10 genes. The RT-qPCR assays were performed in duplicates at the following conditions: 95 °C/10 min, 40 cycles of 95 °C/30 s, 60 °C/60 s and 72 °C/30 s. Data were captured using Stratagene MxPro Mx3000P QPCR software. Melting curve analysis resulted in single peak for each primer set.

Statistical analyses

All the statistical analyses were done manually by means of Student *t*- test. The *p*- values < 0.05 were identified as significant and were reported.

Results

ISAV s8ORF2 shows RNAi-suppression activity in *in planta* assay

In order to investigate the RNAi-suppression activity of s8ORF2 protein, we employed a popular *in planta* assay wherein s8ORF2 gene was cloned in a plant expression vector pBI121 along with SARS-7a, SARS-3a (positive control), and SARS-6a (negative control, [36]). All DNA samples were agroinfiltrated onto GFP-silenced leaf (in

Table 1 Forward (F) and reverse (R) primers used in this study

Gene	Sequence 5′–3′	GenBank accession no.
EF1αB	F-TGCCCCTCCAGGATGTCTAC	BG933897
	R-CACGGCCCACAGGTACTG	
	P-FAM-AAATCGGCGGTATTGG-MGB-NFQ	
ISAV seg8	F-CTACACAGCAGGATGCAGATGT	AY151791
	R-CAGGATGCCGGAAGTCGAT	
	P-FAM-CATCGTCGCTGCAGTTC-MGBNFQ	

triplicates) of T2 (second-generation tobacco plants) stable line of *Nicotiana xanthi* [36, 43]. Agroinfiltration of a test ORF would lead to its transient expression *in planta* where its activity is studied. The agroinfiltrated leaves were collected 7 days post-infiltration (dpi) and observed over UV trans-illuminator in darkroom. The GFP-silenced leaf and SARS-6a-infiltrated leaf appeared red under UV due to chlorophyll auto-fluorescence [44] whereas the s8ORF2 appeared fluorescent green similar to the positive controls SARS-7a and SARS-3a (Fig. 1a). Thus, the expression of s8ORF2 in the GFP-silenced line resulted in the reversal of silencing effect and thereby restored the expression of previously silenced reporter gene GFP. Hence, ISAV-s8ORF2 acts as a suppressor of RNA silencing, *in planta*.

The s8ORF2 protein is responsible for the RNAi-suppression activity in vitro

To ascertain the RNAi-suppression activity of s8ORF2, we next used GFP-silenced mammalian HEK293T cells. We

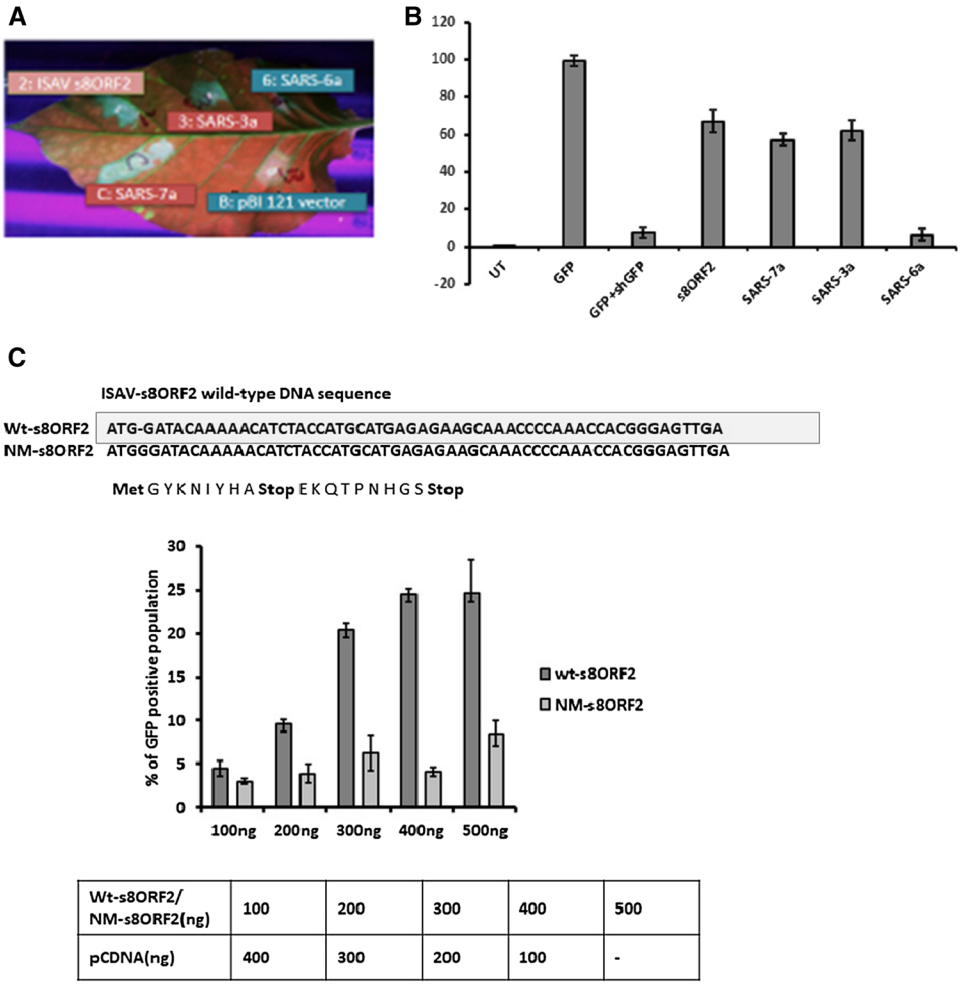

Wt-s8ORF2/ NM-s8ORF2(ng)	100	200	300	400	500
pCDNA(ng)	400	300	200	100	-

Fig. 1 s8ORF2 functions as a VSR. **a** Reversal of silencing assay to determine the VSR activity of ISAV s8ORF2. A GFP-silenced leaf was agro-infiltrated with different constructs and observed over UV trans-illuminator after 8dpi. Patches of green fluorescence was observed in zones agro-infiltrated with ISAV s8ORF2 similar to the positive controls SARS-7a and SARS-3a. Whereas, rest of the leaf as well as the regions agro-infiltrated with empty vector and negative control SARS-6a remained red due to chlorophyll auto-fluorescence. **b** RNAi suppression by ISAV s8ORF2 in HEK-293 T cells using a transient silencing suppressor assay. Cells were transfected with plasmids expressing GFP, GFP shRNA and ISAV s8ORF2 and quantified for GFP-positive cell population using flow cytometry. The GFP, SARS-3a and SARS-7a were used as positive controls and GFP + shGFP and SARS-6a as negative controls; s8ORF2 shows reversal of GFP by 67%, the SD value of 8%. The data are obtained from four experiments performed in triplicates **c**. Designing of Non sense-mutant by insertion of G after methionine. The insertion of G at this strategic point expels in-frame protein expression from first Methionine. **d** Dose-dependent analysis (of the s8ORF2 protein and its NM-s8ORF2 mutant) of RNAi suppression in HEK-293 T cells using a transient silencing suppressor assay. Cells were transfected with increasing amount of plasmid and GFP content were analysed by flow cytometry. The GFP-positive cells were quantified as 96.91% with the SD value of 1.032 (not shown in the plot). X-axis depicts FL1 fluorescence, Y-axis depicting the percentage of GFP-positive cells. The individual *p*-values calculated by student *t* test were < 0.05. The experiments were done in triplicates (and repeated thrice) results analysed using winMDI software

conducted transient RNAi suppression (Fig. 1b) as indicated in previous reports [36], and quantified GFP reversal. The graph (Fig. 1b) shows population of HEK293T cells exhibiting reverted GFP-expressing cell population in the range of approximately 67% for s8ORF2, as against GFP silenced (7.8%). SARS-7a and SARS-3a were used as positive controls. In Adenovirus VA, the RNA molecules, RNAI and RNAII have been identified to be responsible for the RNAi suppressor function [45, 46]. To elucidate the role of s8ORF2 protein versus *s8orf2* RNA in the RNAi-suppression assay, a nonsense mutant was generated by inserting a base (G) immediately after the start codon using site-directed mutagenesis (Fig. 1c). This nonsense mutant was termed NM-s8ORF2. Dose-dependent analyses of s8ORF2 and NM-s8ORF2 were done by incrementing the amount of DNA by 100 ng in each well. The addition of wt-s8ORF2 plasmid in increasing concentration, increased the suppression, reflected by increase in the population of GFP-positive cells from 5% with 100 ng to 25% with 500 ng (Fig. 1c). The NM-s8ORF2 had minimal influence on GFP-expressing population, with a maximum effect at ~ 5.5% with (500 ng) suggesting that the VSR activity is a component of s8ORF2 protein but not its RNA, which was otherwise conserved in NM-s8ORF2.

The s8ORF2 protein binds to RNA molecules in vitro

In order to explore the RNA-binding capacity of s8ORF2 in suppressing the RNAi pathway, we carried out Electrophoretic Mobility Shift Assay (EMSA). Bacterially purified s8ORF2-GST and GST were assayed for their siRNA-binding activities in the presence of 21 bps GFP siRNA. Alongside, an already studied *Mung*bean *Yellow* Mosaic India *Virus (*MYMIV) protein AC-2 fused to MBP was used as a negative control. MYMIV is a VSR but devoid of siRNA-binding activity [47]. The results showed no change in the mobility of GFP probe on incubation with GST, MBP and AC2-MBP proteins, whereas with s8ORF2, probe mobility was significantly reduced, suggesting that s8ORF2 possesses siRNA-binding activity (Fig. 2a). We validated the s8ORF2–siRNA complex band by increasing the s8ORF2 protein amount from 37.5 to 75.0 µmol/L and 150.0 µmol/L. We observed a continued increase in the intensity of a specific band with increased dose (Fig. 2b lane 3–5). Since no further increase in the intensity was observed subsequent to increase from 75.0 to 150.0 µmol/L, we used 75.0 µmol/L of s8ORF2 for all further experiments. In supershift experiments, shift in the band with anti-s8ORF2, but not with anti-His (non-specific ab) (Fig. 2b, lane 6–7) confirmed the specificity of the s8ORF2-siRNA band.

Further, we tested for specific binding of s8ORF2 to single- or double-stranded RNA and DNA oligos. In a competition EMSA (RNA or DNA molecules compete for binding with test protein incubated previously with labelled oligos), unlabelled oligos were added along with the labelled siRNA in amounts 25 and 50 × higher than that of the latter. Both 21-bp single-stranded (ss) and double-stranded (ds) RNAs were able to compete for binding to s8ORF2-GST, as observed by reducing intensities of the corresponding complex band (Fig. 2c lane1-6), while ds and ss DNAs did not show competition (lane 7–10), explicitly showing indiscriminate binding towards RNA molecules but not to DNA molecules (Fig. 2c).

We also investigated whether s8ORF2 could bind to long RNA molecules (300 bp) and hence performed a competition EMSA with 300-bp-long RNA molecules obtained using in vitro transcription kit. Competitive binding assay of s8ORF2 with unlabelled long ss and ds RNAs were run to find the specificity of binding in two different concentrations, i.e. 25 × and 50 × as shown in Fig. 2d. Both ss and ds RNAs of ~ 300-bp oligonucleotides were able to compete for binding to s8ORF2-GST.

These experiments confirmed that s8ORF2 has RNA-binding activity towards ss and ds RNAs, ranging from 21 to 300 bp in length.

Functional domain and motif analysis of s8ORF2

RNA-binding activity of s8ORF2 is present in region spanning 62 aa-195 aa

To map the RNA-binding region in the s8ORF2 gene, we used BIND-N software, which predicted an RNA-binding domain at the N-terminus (1-61 amino acids) of s8ORF2 [48]. Also using COILS Software [8], a coiling domain was predicted to be present in the C-terminal of s8ORF2 spanning 196–243 aa (illustrated in Fig. 3a) [8]. Based on these predictions, we hypothesised that these domains might display the functions of RNA binding and dimerisation and therefore designed deletion mutants and tested them in the RNA-EMSA experiments (Fig. 3b). We generated deletion mutants by PCR amplification, namely, ΔNTD with 183 nt deleted from the N-terminal, ΔCTD with 144 nt deleted from the C-terminus. These were cloned in the pGEX-4T-1 plasmid, and the purified proteins were obtained. Both the truncated polypeptides retained the RNA-binding activity, as shown in Fig. 3b, lanes 1–4. We also made a double-deletion mutant in which both the N- and C-terminals were deleted; we denoted this mutant as ΔDD. These RNA-EMSA experiments mapped the RNA-binding region of S8ORF2 between 62 and 195 aa (Fig. 3b, lane 6).

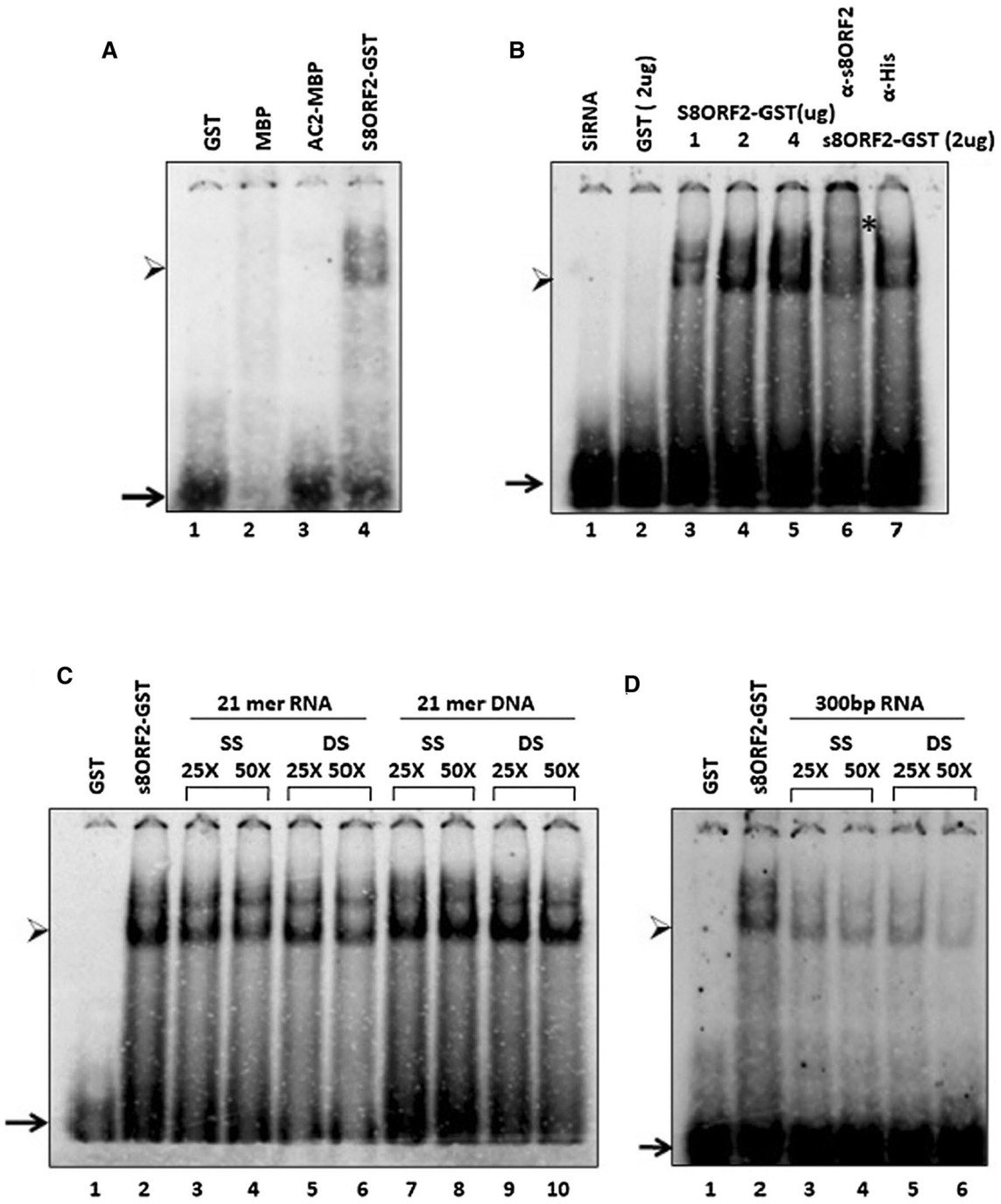

Fig. 2 RNA-binding function of s8ORF2 **a** Analysis of binding of siRNA with s8ORF2 protein and the negative control AC-2 s8ORF2-binding activity was analysed using a negative control AC-2-MBP(MYMIV) and its MBP fusion protein which were used in 2 µg concentration. Purified GST used as negative control for s8ORF2 fusion protein. All proteins were incubated with same concentration of labelled GFP siRNA (0.16 pmol) for 30 min and subsequently run on 6% PAGE. **b** The Dose-dependent increase in binding of siRNA to s8ORF2 by EMSA. s8ORF2 protein-binding standardisations were done using 1, 2 and 4 µg using different concentrations of protein and equal concentration of labelled GFP siRNA (0.16 pmol). Supershift was analysed using anti-ISAV s8ORF2 antibody and anti-His antibody. **c** Competition assay using cold, single- and double-stranded (ss/ds) 21-bp oligonucleotides. Unlabelled RNA/DNA oligonucleotides were taken in singlex or duplex forms, bound to s8ORF2 in 25 and 50 mM excess (4.0 and 8.0 pm) of the labelled siRNA. **d** Competition assay using cold, single- and double-stranded (ss/ds) 300-bp RNA EMSA. Long RNA (300 bp) were taken in singlex or duplex unlabelled forms, and bound to s8ORF2 in 25 and 50 mM excess (4.0 and 8.0 pm) of the labelled siRNA

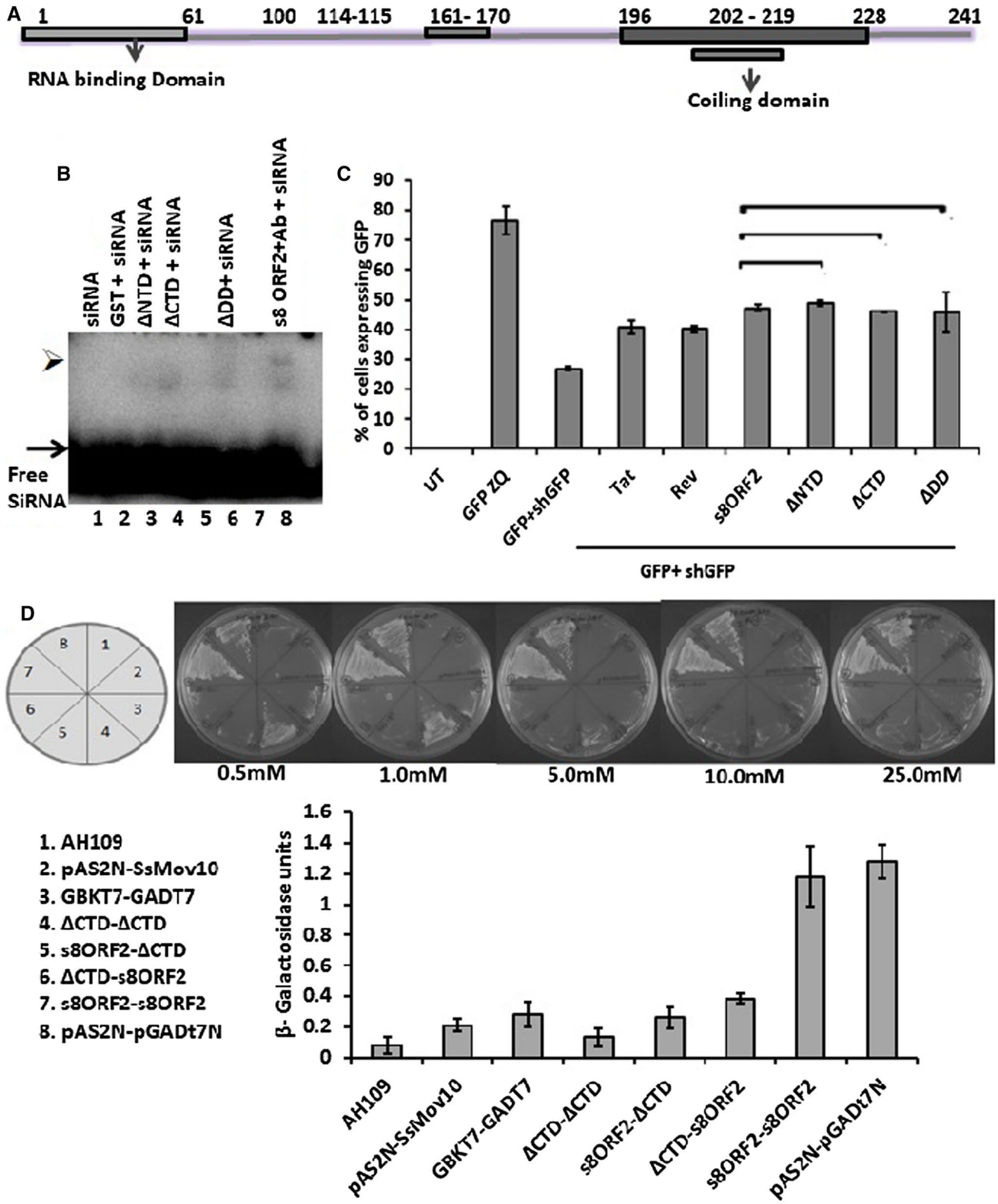
A
1
61
100
114-115
161- 170
196
202 - 219
228
241
RNA binding Domain
Coiling domain
B
siRNA
GST + siRNA
ΔNTD+ siRNA
ΔCTD + siRNA
ΔDD+ siRNA
s8 ORF2+Ab + siRNA
Free SiRNA
1 2 3 4 5 6 7 8
C
% of cells expressing GFP
UT
GFP ZQ
GFP+shGFP
Tat
Rev
s8ORF2
ΔNTD
ΔCTD
ΔDD
GFP+ shGFP
D
0.5mM
1.0mM
5.0mM
10.0mM
25.0mM
1. AH109
2. pAS2N-SsMov10
3. GBKT7-GADT7
4. ΔCTD-ΔCTD
5. s8ORF2-ΔCTD
6. ΔCTD-s8ORF2
7. s8ORF2-s8ORF2
8. pAS2N-pGADt7N
β- Galactosidase units
AH109
pAS2N-SsMov10
GBKT7-GADT7
ΔCTD-ΔCTD
s8ORF2-ΔCTD
ΔCTD-s8ORF2
s8ORF2-s8ORF2
pAS2N-pGADt7N

◂**Fig. 3** Domain mapping of s8ORF2 functions. a. Bio-informatic prediction (BindN) of RNA-binding domains of ISAV s8ORF2 and (COILS) coiling domains for dimerisation N- and C- terminal domains were deleted, and mutants were cloned in pCDNA3.1 plasmid, pGEX4T-1 pGBKT7 and pGADT7 vectors for experiments in the respective systems. The numbers at the ends of the deletions refer to amino acids. The stop codons were introduced during cloning (start codon was a part of expression vector). **b** Analysis of binding of siRNA with wt-s8ORF2 protein and the deletion mutants, ΔNTD, ΔCTD and ΔDD. The binding activity was analysed using a negative control GST, all of which were used in 2 µg concentration. **c** RNAi-suppression analyses of wt-s8ORF2, ΔNTD, ΔCTD, ΔDD, deletion mutants. GFP contents were analysed by flow cytometry. The GFP-positive cells were quantified, and p-values were calculated using student *t*-test, > 0.05. X-axis depicts FL1 fluorescence, Y-axis depicting the percentage of GFP-positive cells. The experiments were done in triplicates. Each experiment was performed thrice, N = 3, and results analysed using winMDI software. **d** Dimerisation domain resides in C-terminal. As shown, numbered with the quadrants. quadrant 1:AH109 (negative transformation control); 2: pAS2 and SsMov-10 (non-interacting partners, therefore, negative control); 3: GBKT7-GADT7 (empty vectors, therefore negative control); 4: ΔCTD (GBKT7 vector)- ΔCTD (GADT7 vector); 5: s8ORF2 (GBKT7 vector)- ΔCTD (GADT7 vector); 6: ΔCTD (GBKT7 vector)-s8ORF2 (GADT7 vector); 7: S8ORF2 (GBKT7 vector) -s8ORF2 (GADT7 vector); and 8: N (AS2vector)-N (GADT7 vector) which is a previously published interacting positive control. *3-Amino Triazole competition assay* as explained above (clockwise from centre position), where AH109 is the negative transformation control yeast cells, and pAS2 N and SsMov-10 are the negative interaction controls, and N–N is the positive interaction controls. *Liquid beta gal assay* the values of pAS2 N-pGADT7 N dimer (1.28) and s8ORF2-s8ORF2 dimers (1.182) which clearly specify the interaction occurring (mean ± SD, done in triplicates, and the experiment done thrice) in the C-terminal and is abolished if the C-terminal is deleted (p-value < 0.05)

RNAi-suppression function is present in the middle region (62–195 aa) of s8ORF2

It is speculated that the RNA-binding domain is responsible for the RNAi-suppression activity since it sequesters RNA molecules of the pathway. After having shown that RNA binding is present in the middle region of s8ORF2, we attempted to understand the region responsible for RNAi-suppression activity. We cloned the respective fragments in the pcDNA3.1 vectors (in *Eco*RI and *Bam*HI sites) and used the three deletion mutants, i.e. ΔNTD, ΔCTD and ΔDD in the GFP-reversal assay (already described). In this assay, the RNAi-suppressing activity of a test protein results in the increase in GFP-expressing cells population. Since all three mutants could revert the percent of GFP-positive population as s8ORF2 (Fig. 3c), we inferred that both the N- & C-terminals were dispensable for this role.

Therefore, the RNAi-suppression activity is localised to the middle region spanning 62–195 aa. Tat and Rev (HIV-1) were used as positive controls, already reported from previous publications from our group [49].

The dimerisation domain of s8ORF2 is localised at the C-terminal region

Using the COILS protein domain prediction software, the C-terminal amino acids (196–243 aa) were predicted for dimerisation [8]. The dimerisation capacity of most RNAi suppressor molecules identified, has been established, and is speculated to be responsible for their activity. Therefore we tested the C-terminal deletion mutants for dimerisation in a yeast two-hybrid assay. The truncated s8ORF2 was made to interact with C-terminal deletion (ΔCTD) on both GBKT7 and GADT7 vectors, respectively. Similarly the pGBKT7-ΔCTD and pGADT7-ΔCTD were also tested for dimerisation in the yeast two-hybrid assay. The doubly deleted ΔCTD-ΔCTD produced no colonies whereas s8ORF2-s8ORF2 (both wild type protein in respective vectors) produced colonies as well as blue colour in Beta-galactosidase assay, indicating positive dimerisation (Fig. 3d). Therefore, the C-terminal carries the dimerisation domain confirming our COILS prediction [8]. But we could not find any difference in the RNAi-suppression activity of the three deletion mutants as indicated by p-values (Fig. 3c).

In vitro analysis of GW motif points display a significant role in RNAi suppression

Glycine-tryptophan motifs have been identified in RNAi suppressor proteins, with the motif being essential for binding Argonaute-2 [50]. s8ORF2 has a GW motif at $_{114}$GW$_{115}$ (Fig. 4a). To elucidate the role of this motif in s8ORF2, we mutated it to $_{114}$GA$_{115}$, in the wt-s8ORF2 and named s8ORF2 GA. s8ORF2 GA had significantly declined levels of RNAi-suppression activity as assessed in GFP-reversal assay, i.e. from 47.5 to 35.8%. At this conjecture, the nominal decline in GFP-reversal activity of the s8ORF2 GA mutant suggests the possible involvement of other molecules of the RNAi machinery, besides the Ago-2, with which s8ORF2 might interact to effectively suppress RNAi (Fig. 4b).

s8ORF2 interacts with SsMov10, an endogenous VSR

In order to identify proteins of the RNAi machinery which interact with s8ORF2, we utilised phage display. The purified s8ORF2 protein was used as bait in a 96 well plate and phage library was exposed to the bait according to the manufacturer's protocol. This screen identified a number of RNAi co-factors as putative interactors. We selected SsMov10 [51, 52] as a potential interactor using Informatic tools. SsMov10 is a RNA helicase component of the RNAi pathway and is actively involved in post-transcriptional gene silencing (PTGS). Recently it has been identified as a host restriction factor for the influenza A virus life cycle across

various species [53]. In the yeast two-hybrid assay the interaction was found to be strong enough to withstand 25 mM 3-Amino Triazole (Fig. 5a, quadrant 5) and showed fivefold higher β-galactosidase activity as compared to the controls (Fig. 5a β-galactosidase activity histogram). Interestingly, ΔNTD-s8ORF2 exhibited even higher strength of interaction with SsMov10 (Fig. 5a, quadrant 6 and 5a β-galactosidase activity histogram). Mutant studies revealed that s8ORF2 requires the C-terminal for this interaction as ΔCTD did not show interaction with SsMov10 (Fig. 5a quadrant-7 and 5a β-galactosidase activity histogram). To supplement this analysis, we also identified the co-localisation between SsMov10 and s8ORF2 using immunofluorescence (Fig. 5b).

SsMov10 functions as an s8ORF2 aide

We began with analysing the involvement of SsMov10 in ISAV infection. We looked at the endogenous mRNA levels of SsMov10 on ISAV infection in TO cells. Real-time qPCR analysis of cellular mRNA levels showed a spike elucidating elevation of SsMov10 expression, 6 hpi (Fig. 5d (i)). To our surprise, the level of SsMov10 declines to normal physiological concentration with completion of viral replication and counter-defence cycle at 72 hpi (Fig. 5d (i)).

To understand the role of SsMov10 in the RNAi pathway, we assayed it for mammalian RNAi suppression (in vitro). On overexpressing in HEK293T cells, surprisingly, the SsMov10 was found to suppress the RNAi pathway quite

Fig. 5 In vitro analysis of SsMov10 activity in RNAi suppression. **a** ▶ SsMov10 interaction domain resides in C-terminal of s8ORF2 The yeast two-hybrid assays were performed according to the Manufacturer's protocol, Clontech Manual Gal-4 system in AH109 yeast *Saccharomyces cerevisiae* strain. All the three assays were performed for reliability and were done in triplicates (the quadrants are mentioned against their numbers), where AH109 is the negative control yeast cells, and pAS2 N and SsMov-10 as the negative interaction controls. The data are from 3 independent experiments. **b** Confocal microscopy shows co-localisation of s8ORF2 and SsMov10. Transfected EPC cells express both SsMov10 (green) and ISAV s8ORF2 (red) in the cytosol, showing co-localisation. Pictures captured in confocal microscope at 63x magnification. Scale bar = 10 μM. Controls are untransfected cells immunostained with the same antibodies, and pictures were taken with the same intensity settings. The co-localisation was repeated thrice. **c** GFP reversal and Role of SsMov-10 in reversing GFP. HEK293T cells transfected with the SsMov10 +s8ORF2 show enhanced level of GFP reversal. GFP-expressing cell population was analysed by flow cytometry. The data are shown as mean ± SD of three independent experiments (done in duplicates). $*p < 0.05$. **d** (i): Real-time qPCR analysis of time-dependent SsMov10 and s8ORF2 expressions during infection with ISAV in TO cells. Expression of SsMov10 results in a spiked increase from endogenous 0.03 value at 0 h to 0.72 at 6 h, and then declines to lower endogenous levels with ISAV infection with a 1:10 dilution of TCID50/25 μl with viral titre $5 \times 10^{6.25}$. **d** (ii): Real-time qPCR analysis of dose-dependent SsMov10 and s8ORF2 expressions on infection with serially diluted ISAV titres in TO cells. The TO cells were infected with 1:10 serially diluted supernatant. The TCID50/25 μl value for the undiluted supernatant is $5 \times 10^{6.25}$. The cells (TO) were infected with the (1) undiluted supernatant, and with the following dilutions: (2) 1:10, (3) 1:100, (4) 1:1000, (5) 1:10 000, and results were plotted using log scale. The cells were harvested at 24 h post infection (hpi). These data are from one experiment run in triplicate

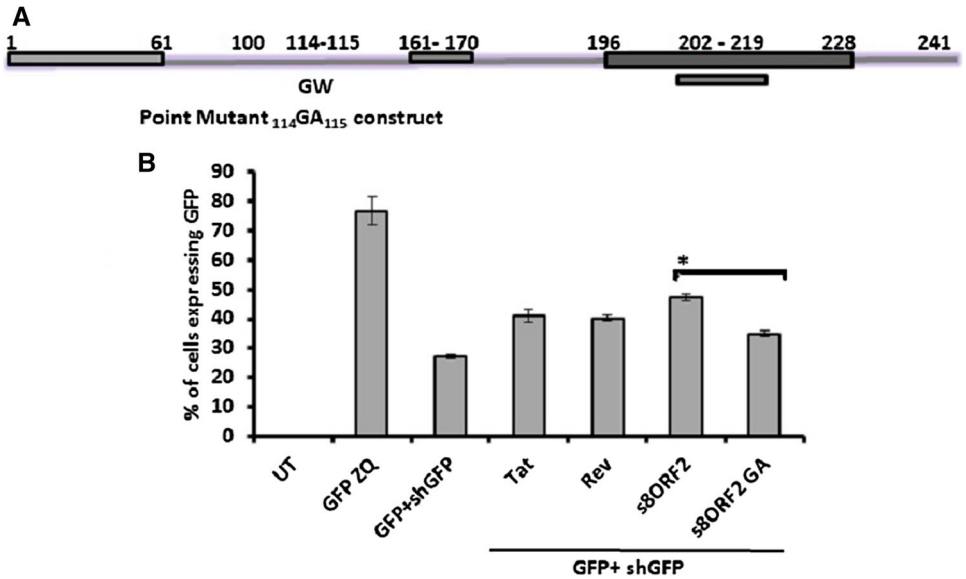

Fig. 4 Role of GW motif in RNAi suppression **a** Site-directed mutagenesis of $_{114}GW_{115-114}GA_{115}$ The GW domain of a protein is categorically identified as an Ago-hook, is found in most RNAi suppressors and is crucial for RNAi suppression. It was identified and mutated to GA, by site-directed mutagenesis and cloned in pcDNA vector at *Eco*RI and *Bam*HI sites. **b** s8ORF2 $_{114}GW_{115}$ mutant has significantly lowered RNAi-suppression activity in GFP-reversal assay. GFP-reversal assay was performed for the GW mutant, using HIV-1 Tat and Rev as positive controls for the activity. The mutant showed decline in activity. The *p*-value calculated using student *t*-test was $*p < 0.05$. The experiment was done in duplicates and repeated thrice

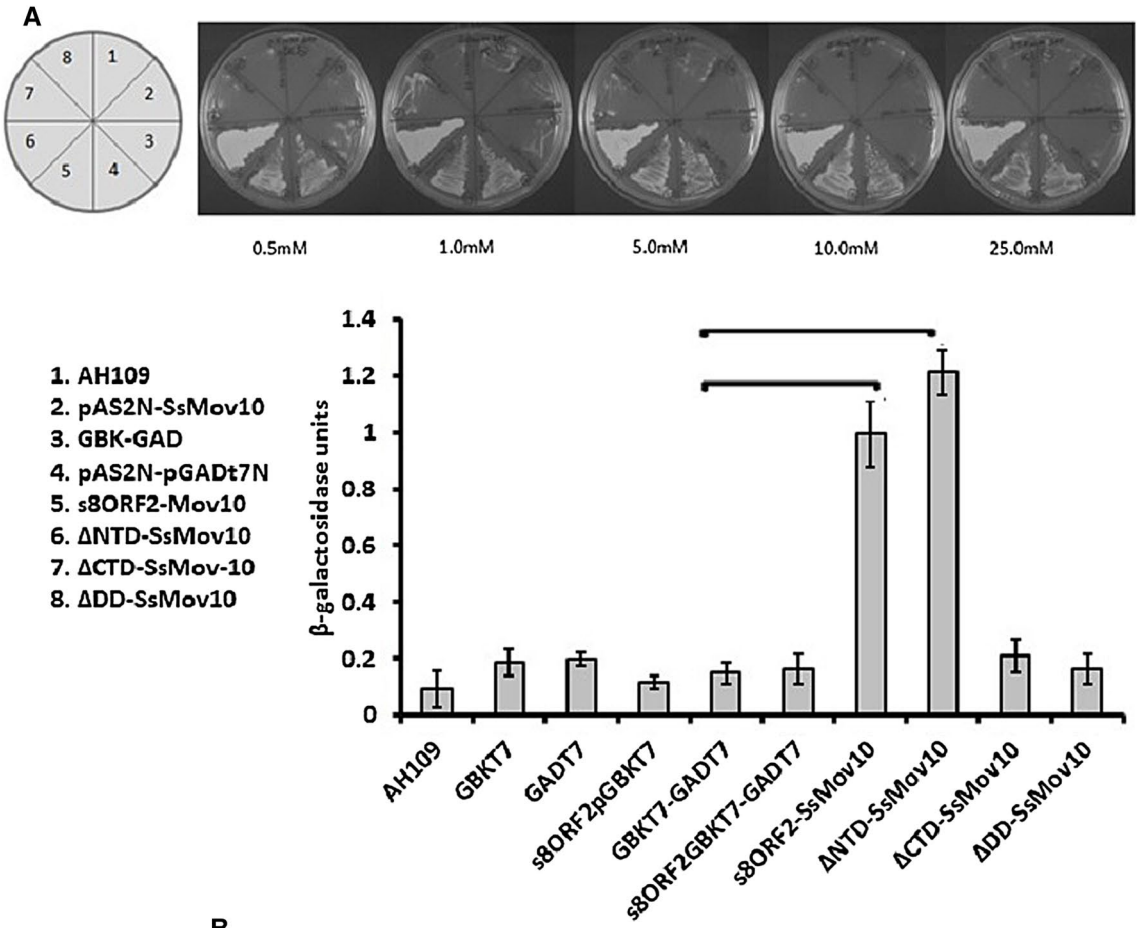

equivalent to that of s8ORF2 (Fig. 5c), indicating that it may also possess RNAi-suppression activity. On co-transfecting s8ORF2 and SsMov10, in the GFP-reversal assay, we found enhanced GFP reversal compared to cells transfected individually with s8ORF2 or SsMov10 (Fig. 5c), suggesting that SsMov10 may supplement the RNAi suppressor function of s8ORF2 endogenously. To support this hypothesis, we performed real-time qPCR experiments in infected TO cells. The physiological concentration of SsMov10 was estimated by real-time qPCR experiments, taking the EF factor as a control. These values were used as a reference for further analysis of correlation in the expression of the

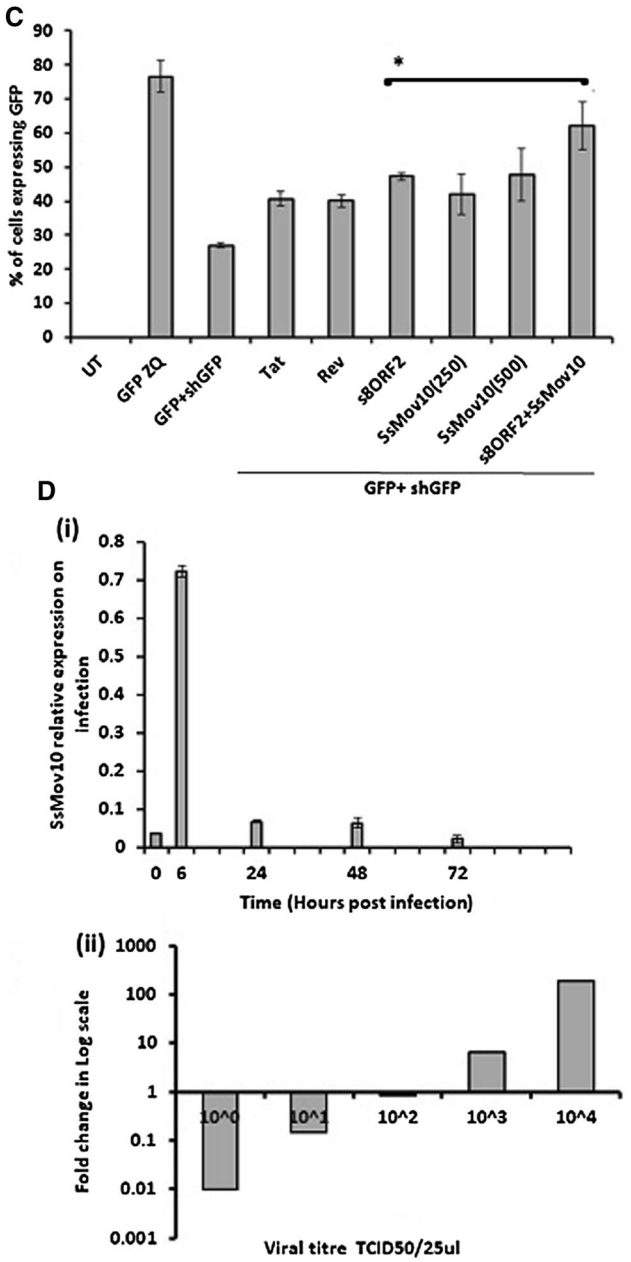

Fig. 5 (continued)

ISAV s8ORF2 protein with infection. However, these results should be supported and substantiated with siRNA-based silencing experiments (to silence endogenous SsMov10), but we were constrained due to the low transfection efficiency of TO cells, to carry out our experiments.

Logically, as in the mechanism of VSR proteins, we were interested to know, if s8ORF2 protein utilised SsMov10 through transcriptional control as well. It is evident in Fig. 6d (i) that the level of SsMov10 declines at about the end of viral replication cycle as well. These results suggest regulation of SsMov10 levels during the viral infection at 72 hpi (Fig. 5d (i)). This could be the result of a constant check to prevent the protein from engaging in RISC Assembly, since the SsMov10 possesses RISC Assembly function [53]. Next, we analysed the effect of viral dose on SsMov10 transcript levels, which indicated a positive correlation of SsMov10 expression, at 12 hpi, the trend coherently visible even on increasing viral dose (Fig. 5d (ii)). On increasing the viral titre successively by tenfold, there was an increased expression of SsMov10, in comparison with controls (not shown to avoid confusion). We observed a logarithmic scale turnover, in the values of SsMov10 expression, at least at mRNA levels. This trend leads us to hypothesise that a transcriptional control over SsMov10 (Fig. 6), one of the crucial RNAi molecules, is present.

Discussion

In plants, insects and higher animals, RNAi is present as a viral defence mechanism [19, 26, 54–56]. Therefore, screening for RNAi suppressors among viral polypeptides has been widely undertaken to identify the polypeptides which possibly are RNAi pathway interactors. In an established reversal of silencing assays *in planta*, we screened ISAV polypeptides for RNAi-suppression activity, and identified s8ORF2 of ISAV as a potent viral suppressor of RNAi.

In a previous study of two ISAV ORFs for accessory polypeptides, i.e. s7ORF1 and s8ORF2 [8], both were functionally found to be IFN antagonists. The s8ORF2 protein was shown to bind to RNA in a dot–blot assay [8]. In the literature, RNA binding and interferon antagonism have been minimal requirements for recognition as a Viral Suppressor of RNAi protein. The viral protein which exhibits both functions has been shown to function as an RNAi suppressor as well, as identified for E3L of Vaccinia virus, followed by NS1 of Influenza A Virus and then Tat of HIV-1 [32, 56, 57], where all these candidates exhibited both RNA binding and interferon antagonism. Consequently, with the leads of RNA-binding activity [8] and interferon antagonism [8, 58], RNAi suppression was quite well studied.

Therefore, the foremost goal was to identify the specificity of s8ORF2 binding. We have identified that s8ORF2 binds to siRNA as well as long RNA molecules, in the competitive EMSA experiments, in vitro. Here, we can speculate that it binds to the substrates of DICER and RISC in fish cells as well, presuming that this pathway is conserved in fish, similar to its conservation through plants, insects and mammals. We can warrant that since 22 bp and 300 bp are substrates to RNAi pathway, these RNA molecules point to site of s8ORF2's action [59–61]. The VSR protein binding to ds RNA would seize the input of ds RNA to DICER in the RNAi pathway (Fig. 6), thereby paralysing the pathway, as is

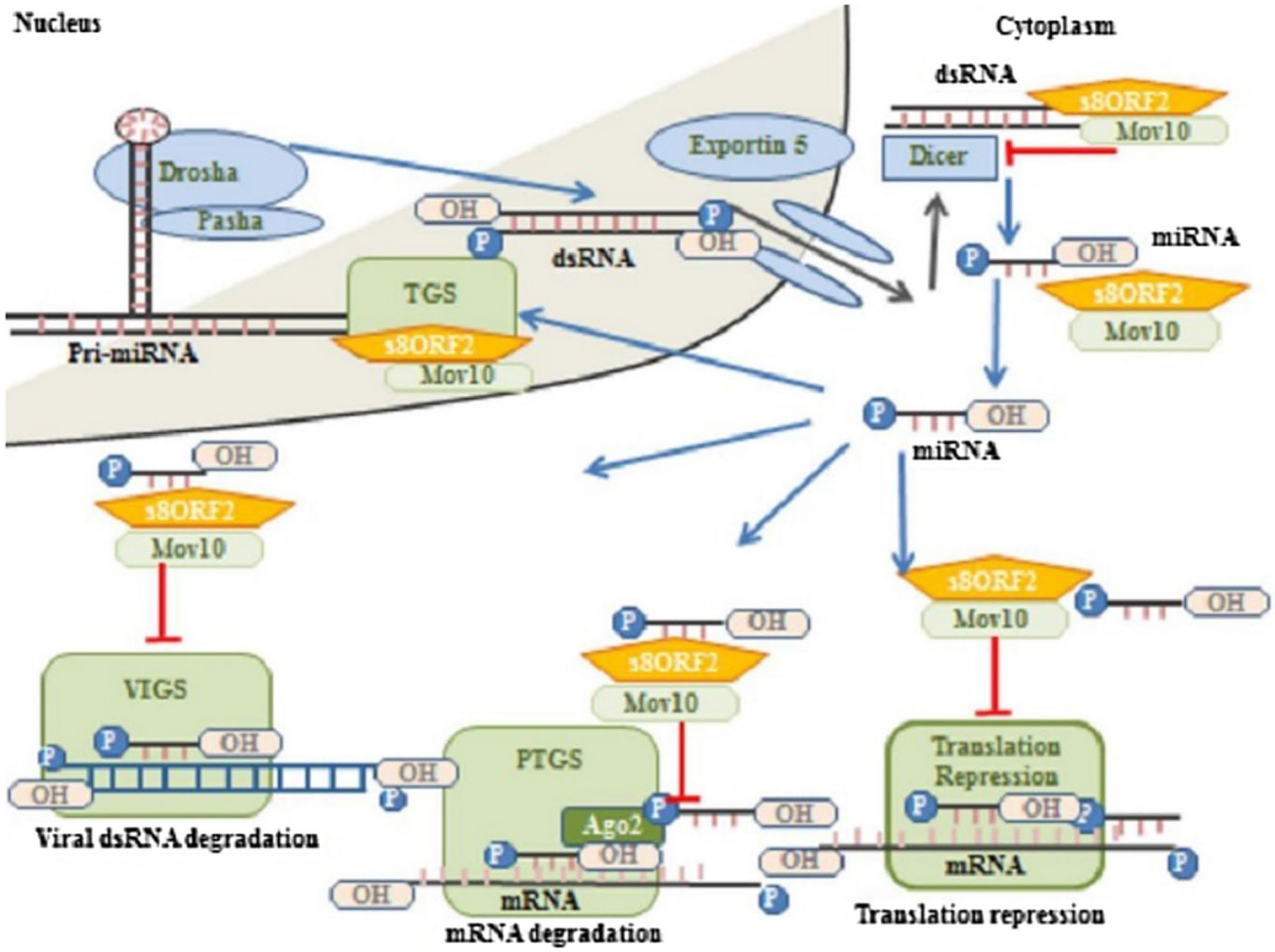

Fig. 6 Graphic representation of the s8ORF2, in the various pathways s8ORF2, depicted as RNAi suppressor molecule. Based on our results, we predict s8ORF2 to be involved in the following pathways: Transcriptional Gene Silencing (TGS), Post Transcriptional Gene Silencing (PTGS), Virus-Induced Gene Silencing (VIGS) and Translational Repression. Since there is a modulation of SsMov10 expression, we predict the innate RNAi response getting stimulated

the case with VP35 (Ebola virus), NS1 (Influenza A virus), B2 (Nodamura virus) and E3L (Vaccinia virus).

In a previous publication, it was hypothesised bio-informatically that there might be specific domains for RNA binding and dimerisation [8]. Thus, we proposed that these functions might exist as independent domains, and cloned three deletion mutants: the first, in which the N-terminal, predicted to be RNA-binding domain (ΔNTD); second, the C-terminal predicted to cause dimerisation (ΔCTD); and third, both N- and C-terminals were deleted (ΔDD). Each of these deletion mutants was analysed for RNA binding, dimerisation and GFP-reversal activity. The RNA-binding activity was found to be focussed in the middle region (62–195 aa). The dimerisation domain was found to be present in the C-terminal but was not responsible for the RNAi-suppression activity. Therefore, we conclude that the RNAi-inhibition-active domain is present in the middle region (62–195 aa), which is doubly deleted for N- and C-terminals. It also has an Ago-binding GW motif at $_{114}$GW$_{115}$. The VSR polypeptides utilise this motif as a hook to seize the Ago-2 molecule and eventually RNAi pathway by selectively targeting host RNA for degradation and favouring vRNA for replication. This implied the presence of another host molecule interacting with s8ORF2, which provisionally aided it in countering the RNAi pathway.

In the case of VSR proteins, it is a well-observed fact that the viral Suppressor proteins induct a protein factor, besides the RNA molecule, of the RNAi pathway, to suit its function of blocking the RNAi pathway. To scrutinise and approach such a factor, we employed Ph.D.-12, Phage display peptide library kit biopanning technique (New England Biolabs Inc., Beverely, MA, USA). We selected SsEPC-1, SsEPC-2, SsMov10 and SsMLL-1 of RNAi pathway (since they were partially identical with 12-bp peptide),

analysed them bio-informatically from the protein library and performed yeast two-hybrid analysis by interacting with s8ORF2. SsMov10 was selected for further analysis, since it was the most studied and belonged to PTGS, whereas other molecules belonged to TGS. SsMov10 was found to interact with s8ORF2 in all the yeast two-hybrid assays, with the C-terminal domain responsible for the interaction. Yeast two-hybrid assay and confocal microscopy confirmed the interaction. Surprisingly, SsMov10 was found to exhibit RNAi-suppression activity. On co-transfecting s8ORF2 and SsMov10 in the same GFP-reversal experiment, their activity was additive, suggesting a clever utilisation of host factor for the viral benefit (Fig. 6).

However, real-time qPCR analysis (Fig. 5d (i)) of SsMov10 transcript levels in infected cells unveiled a second level of regulation, i.e. transcriptional control over SsMov10 levels by viral protein. Interestingly, at 0–6 h, the expression of SsMov10 mRNA increased, and from 6 to 24 h, it declined sharply, on virus infection. Mov10 interactions with viral proteins have also been reported elsewhere [62]. From 0 to 6 h, when the virus uncoats and releases the RNA–protein complex, SsMov10 is logically expected to be required at higher endogenous levels to combat the viral replication. From 6 to 18 h, the s8ORF2 is transcribed, translated and enters the nucleus [8, 58].

We understand that our experiments are limited in Western blot data (which is because of the antibody for Mov10 of human origin does not identify endogenous SsMov10), and transfection deficiencies of TO cell lines (for probing with overexpressed tagged SsMov10). TCID50/25 µl value given on the X-axis, in the dose-dependence real-time qPCR experiment, indicates a positive correlation of SsMov10 mRNA expression levels, with the increasing viral titres (Fig. 5d (ii)).

Considering homologous function (of RISC maturation) in piscine cells, the interaction of s8ORF2 with SsMov10 seems to be highly strategic for inhibiting the RISC assembly (Fig. 6). Since there is a modulation of SsMov10 expression, it becomes undisputed that the innate RNAi response begins with temporally enhanced transcription of SsMov10 RNA expression by unknown transcription factors. It also implies that the TGS pathway factors which have been identified by us, using phage display technique, stand a bright chance for further analysis in this pathway for regulating the SsMov10 expression through feedback loop.

Acknowledgements This research was funded by the Department of Biotechnology Indo-Norwegian grant, Govt. of India; the Indian Council for Medical Research fellowship for VT, research grant 183196/S40 from the Research Council of Norway, and internal funds from the School of Science, Monash University Malaysia. The authors are grateful for technical help from Stine Braaen.

Authors' Contributions SKL, ACB and SKM conceived, designed the experiments. VT and BV performed the EMSA experiments and analysed the results. VT designed and analysed Mutants in EMSA, GFP-reversal assay Phage display and Yeast two-hybrid analysis. VT has written the manuscript. SSP performed Dose-dependent analysis of the s8ORF2 protein, its NM-s8ORF2 mutant and other mutants. SKMi performed the experiment to establish s8ORF2 as a suppressor in GFP-silenced *N. xanthi* in Reversal of Silencing leaf assay. RBR performed and analysed fish cell studies and participated in writing the manuscript. CMO and ER planned the fish cell study and contributed to writing the manuscript. CMO analysed the EPC data and performed the WB and immunostaining concerning NM-s8ORF2. SKL, RZ, ACB and SKM helped in the analysis of the results and editing the manuscript. All co-authors read and approved the final manuscript.

Compliance with ethical standards

Conflicts of interest The authors declare that they have no conflict of interest.

Research involving human participants and/or animals This article does not contain any studies with human participants or animals performed by any of the authors.

Informed consent Informed consent was obtained from all individual participants included in the study.

References

1. McCauley, J.W., Hongo, S., Kaverin, N.V., Kochs, G., Lamb, R.A., Matrosovich, M.N., Perez, D.R., Palese, P., Presti, R.M., Rimstad, E., Smith, G.J.D. Orthomyxoviridae. eds. by M.Q. King, Michael J. Adams, Eric B. Carstens, and Elliot J. Lefkowitz. Virus Taxonomy Classification and Nomenclature of Viruses Ninth Report of the International Committee on Taxonomy of Viruses Editors Andrew 2012. Elsevier 2012
2. O. Evensen, K.E. Thorud, Y.A. Olsen, A morphologic study of the gross and light microscopic lesions of infectious anaemia in Atlantic salmon (*Salmo salar*). Res. Vet. Sci. **51**(2), 215–222 (1991)
3. T. Hovland, A. Nylund, K. Watanabe, C. Endresen, Observation of infectious salmon anaemia virus in Atlantic salmon, Salmo salar L. J. Fish Dis. **17**, 291–296 (1994)
4. K.E. Thorud, H.O. Djupvik, Infectious salmon anemia in Atlantic salmon (Salmo salar L.). Bull. Eur. Assoc. Fish Pathol. **8**, 109–111 (1988)
5. S.C. Clouthier, T. Rector, N.E. Brown, E.D. Anderson, Genomic organization of infectious salmon anaemia virus. J. Gen. Virol. **83**(Pt 2), 421–428 (2002)
6. K. Falk, V. Aspehaug, R. Vlasak, C. Endresen, Identification and characterization of viral structural proteins of infectious salmon anemia virus. J. Virol. **78**(6), 3063–3071 (2004)
7. S. Mjaaland, E. Rimstad, K. Falk, B.H. Dannevig, Genomic characterization of the virus causing infectious salmon anemia in Atlantic salmon (*Salmo salar* L.): an orthomyxo-like virus in a teleost. J. Virol. **71**(10), 7681–7686 (1997)
8. E. Garcia-Rosado, T. Markussen, Ø. Kileng, E.S. Baekkevold, B. Robertsen, S. Mjaaland, E. Rimstad, Molecular and functional characterization of two infectious salmon anaemia virus (ISAV) proteins with type I interferon antagonizing activity. Virus Res. **133**(2), 228–238 (2008). https://doi.org/10.1016/j.virusres.2008.01.008

9. E. Bierin, K. Falk, E. Hoel, J. Thevarajan, M. Joerink, A. Nylund, C. Endresen, B. Krossøyl, Segment 8 encodes a structural protein of infectious salmon anaemia virus (ISAV); the co-linear transcript from segment 7 probably encodes a non-structural or minor structural protein. Dis. Aquat. Organ. **49**(2), 117–122 (2002)
10. C. Wilkins, R. Dishongh, S.C. Moore, M.A. Whitt, M. Chow, K. Machaca, RNA interference is an antiviral defence mechanism in Caenorhabditis elegans. Nature. **436**(7053), 1044–1047 (2005)
11. H. Bohle, N. Lorenzen, B.D. Schyth, Species specific inhibition of viral replication using dicer substrate siRNAs (DsiRNA) targeting the viral nucleoprotein of the fish pathogenic rhabdovirus viral hemorrhagic septicemia virus (VHSV). Antiviral Res. **90**(3), 187–194 (2011)
12. C.D. Blair, Mosquito RNAi is the major innate immune pathway controlling arbovirus infection and transmission. Future Microbiol. **6**(3), 265–277 (2011). **Review**
13. Ø. Kileng, M.I. Brundtland, B. Robertsen, Infectious salmon anemia virus is a powerful inducer of key genes of the type I interferon system of Atlantic salmon, but is not inhibited by interferon. Fish Shellfish Immunol. **23**(2), 378–389 (2007)
14. S. Schütz, P. Sarnow, Interaction of viruses with the mammalian RNA interference pathway. Virol. **344**(1), 151–157 (2006). **Review**
15. P. Wieczorek, A. Obrępalska-Stęplowska, Suppress to Survive-Implication of Plant Viruses in PTGS. Plant Mol. Biol. Report. **33**(3), 335–346 (2015). **Review**
16. C. Li, L. Greiner-Tollersrud, B. Robertsen, Infectious salmon anemia virus segment 7 ORF1 and segment 8 ORF2 proteins inhibit IRF mediated activation of the Atlantic salmon IFNa1 promoter. Fish Shellfish Immunol. **52**, 258–262 (2016)
17. R.E. Randall, S. Goodbourn, Interferons and viruses: an interplay between induction, signalling, antiviral responses and virus countermeasures. J Gen. Virol. **89**(Pt 1), 1–47 (2008). **Review**
18. A.J. Hamilton, D.C. Baulcombe, A species of small antisense RNA in posttranscriptional gene silencing in plants. Science. **286**(5441), 950–952 (1999)
19. S.M. Hammond, E. Bernstein, D. Beach, G.J. Hannon, An RNA-directed nuclease mediates post-transcriptional gene silencing in Drosophila cells. Nature. **404**(6775), 293–296 (2000)
20. P.V. Maillard, C. Ciaudo, A. Marchais, Y. Li, F. Jay, S.W. Ding, O. Voinnet, Antiviral RNA interference in mammalian cells. Science. **342**(6155), 235–238 (2013)
21. T.P. Chendrimada, R.I. Gregory, E. Kumaraswamy, J. Norman, N. Cooch, K. Nishikura, R. Shiekhattar, TRBP recruits the Dicer complex to Ago2 for microRNA processing and gene silencing. Nature. **436**(7051), 740–744 (2005)
22. B.A. Janowski, K.E. Huffman, J.C. Schwartz, R. Ram, R. Nordsell, D.S. Shames, J.D. Minna, D.R. Corey, Involvement of AGO1 and AGO2 in mammalian transcriptional silencing. Nat. Struct. Mol. Biol. **13**(9), 787–792 (2006)
23. P.D. Zamore, T. Tuschl, P.A. Sharp, D.P. Bartel, RNAi:double-stranded RNA directs the ATP-dependent cleavage of mRNA at 21 to 23 nucleotide intervals. Cell. **101**(1), 25–33 (2000)
24. B. Berkhout, J. Haasnoot, The interplay between virus infection and the cellular RNA interference machinery. FEBS Lett. **580**(12), 2896–2902 (2006). **Review**
25. L. Song, S. Gao, W. Jiang, S. Chen, Y. Liu et al., Silencing suppressors: viral weapons for countering host cell defenses. Protein Cell. **2**, 273–281 (2011)
26. P.C. Haasnoot, D. Cupac, B. Berkhout, Inhibition of virus replication by RNA interference. J. Biomed. Sci. **10**(6 Pt 1), 607–616 (2003). **Review**
27. D. Silhavy, J. Burgyan, Effects and side-effects of viral silencing suppressors on short RNAs. Trends Plant Sci. **9**(2), 76–83 (2004). **Review**
28. W. de Vries, B. Berkhout, RNAi suppressors encoded by pathogenic human viruses. Int. J. Biochem. Cell Biol. **40**(10), 2007–2012 (2008)
29. G. Fabozzi, C.S. Nabel, M.A. Dolan, N.J. Sullivan, Ebolavirus proteins suppress the effects of small interfering RNA by direct interaction with the mammalian RNA interference pathway. J. Virol. **85**(6), 2512–2523 (2011)
30. J. Haasnoot, W. de Vries, E.J. Geutjes, M. Prins, P. de Haan, B. Berkhout, The Ebola virus VP35 protein is a suppressor of RNA silencing. PLoS Pathog. **3**(6), e86 (2007)
31. W.X. Li, H. Li, R. Lu, F. Li, M. Dus, P. Atkinson, E.W. Brydon, K.L. Johnson, A. García-Sastre, L.A. Ball, P. Palese, S.W. Ding, Interferon antagonist proteins of influenza and vaccinia viruses are suppressors of RNA silencing. Proc. Natl. Acad. Sci. USA. **101**(5), 1350–1355 (2004)
32. S. Qian, X. Zhong, L. Yu, B. Ding, P. de Haan, K. Boris-Lawrie, HIV-1 Tat RNA silencing suppressor activity is conserved across kingdoms and counteracts translational repression of HIV-1. Proc. Natl. Acad. Sci. USA. **106**(2), 605–610 (2009). https://doi.org/10.1073/pnas.0806822106
33. B.J. Fenner, W. Goh, J. Kwang, Sequestration and protection of double-stranded RNA by the betanodavirus b2 protein. J. Virol. **80**(14), 6822–6833 (2006)
34. T. Iwamoto, K. Mise, A. Takeda, Y. Okinaka, K. Mori, M. Arimoto, T. Okuno, T. Nakai, Characterization of Striped jack nervous necrosis virus subgenomic RNA3 and biological activities of its encoded protein B2. J. Gen. Virol. **86**(Pt10), 2807–2816 (2005)
35. M.C. Ou, Y.M. Chen, M.F. Jeng, C.J. Chu, H.L. Yang, T.Y. Chen, Identification of critical residues in nervous necrosis virus B2 for dsRNA-binding and RNAi-inhibiting activity through by bioinformatic analysis and mutagenesis. Biochem. Biophys. Res. Commun. **361**(3), 634–640 (2007)
36. S. Karjee, A. Minhas, V. Sood, S.S. Ponia, A.C. Banerjea, V.T. Chow, S.K. Mukherjee, S.K. Lal, The 7a accessory protein of severe acute respiratory syndrome coronavirus acts as an RNA silencing suppressor. J. Virol. **84**(19), 10395–10401 (2010). https://doi.org/10.1128/JVI.00748-10
37. G. Singh, S. Popli, Y. Hari, P. Malhotra, S. Mukherjee, R.K. Bhatnagar, Suppression of RNA silencing by Flock house virus B2 protein is mediated through its interaction with the PAZ domain of Dicer. FASEB J. **23**(6), 1845–1857 (2009)
38. W. Wang, K. Riedel, P. Lynch, C.Y. Chien, G.T. Montelione, R.M. Krug, RNA binding by the novel helical domain of the influenza virus NS1 protein requires its dimer structure and a small number of specific basic amino acids. RNA. **5**(2), 195–205 (1999)
39. P. James, J. Haliaday, E.A. Craig, Genomic libraries and a host strain designed for highly efficient two hybrid selection in yeast. Genetics. **144**, 1425–1436 (1996)
40. H.I. Wergeland, R.A. Jakobsen, A salmonid cell line (TO) for production of infectious salmon anaemia virus ISAV. Dis. Aquat. Org. **44**(3), 183–190 (2001)
41. M. Løvoll, L. Austbø, J.B. Jørgensen, E. Rimstad, P. Frost, Transcription of reference genes used for quantitative RT-PCR in Atlantic salmon is affected by viral infection. Vet. Res. **42**, 8 (2011)
42. P.A. Olsvik, K.K. Lie, A.E. Jordal, T.O. Nilsen, I. Hordvik, Evaluation of potential reference genes in real-time RT-PCR studies of Atlantic Salmon. BMC Mol. Biol. **6**, 21 (2005)
43. G. Brigneti, O. Voinnet, W.X. Li, L.H. Ji, S.W. Ding, D.C. Baulcombe, Viral pathogenicity determinants are suppressors of transgene silencing in *Nicotiana benthamiana*. EMBO J. **17**(22), 6739–6746 (1998)
44. T.M. Burch-Smith, J.C. Anderson, G.B. Martin, S.P. Dinesh-Kumar, Applications and advantages of virus-induced gene silencing for gene function studies in plants. Plant J. **39**(5), 734–746 (2004). **Review**

45. M.G. Andersson, P.C. Haasnoot, N. Xu, S. Berenjian, B. Berkhout, G. Akusjärvi, Suppression of RNA interference by adenovirus virus-associated RNA. J. Virol. **79**(15), 9556–9565 (2005)
46. S. Lu, B.R. Cullen, Adenovirus VA1 noncoding RNA can inhibit small interfering RNA and MicroRNA biogenesis. J. Virol. **78**(23), 12868–12876 (2004)
47. P. Chellappan, R. Vanitharani, C.M. Fauquet, MicroRNA-binding viral protein interferes with Arabidopsis development. Proc. Natl. Acad. Sci. USA. **102**(29), 10381–10386 (2005)
48. L. Wang, S.J. Brown, BindN: a web-based tool for efficient prediction of DNA and RNA binding sites in amino acid sequences. Nucleic Acids Res. **34**, W243–W248 (2006)
49. S.S. Ponia, S. Arora, B. Kumar, A.C. Banerjea, Arginine rich short linear motif of HIV-1 regulatory proteins inhibits dicer dependent RNA interference. Retrovirol. **11**(10), 97 (2013)
50. E.Z. Szabó, M. Manczinger, A. Göblös, L. Kemény, L. Lakatos, Switching on RNA silencing suppressor activity by restoring argonaute binding to a viral protein. J. Virol. **86**(15), 8324–8327 (2012). https://doi.org/10.1128/JVI.00627-12
51. V. Furtak, A. Mulky, S.A. Rawlings, L. Kozhaya, K. Lee, V.N. Kewalramani, D. Unutmaz, Perturbation of the P-body component Mov10 inhibits HIV-1 infectivity. PLoS ONE. **5**(2), e9081 (2010)
52. J.L. Goodier, L.E. Cheung, H.H. Kazazian Jr., MOV10 RNA helicase is a potent inhibitor of retrotransposition in cells. PLoS Genet. **8**(10), e1002941 (2012)
53. J. Zhang, F. Huang, L. Tan, C. Bai, B. Chen, J. Liu, J. Liang, C. Liu, S. Zhang, G. Lu, Y. Chen, H. Zhang, Host protein moloney leukemia virus 10 (MOV10) acts as a restriction factor of influenza a virus by inhibiting the nuclear import of the viral nucleoprotein. J. Virol. **90**(8), 3966–3980 (2016)
54. B.R. Cullen, RNA interference in mammals: the virus strikes back. Immunity. **46**(6), 970–972 (2017)
55. O. Voinnet, C. Lederer, D.C. Baulcombe, A viral movement protein prevents spread of the gene silencing signal in *Nicotiana benthamiana*. Cell. **103**(1), 157–167 (2000)
56. Y.H. Han, Y.J. Luo, Q. Wu, J. Jovel, X.H. Wang, R. Aliyari, C. Han, W.X. Li, S.W. Ding, RNA-based immunity terminates viral infection in adult Drosophila in the absence of viral suppression of RNA interference: characterization of viral small interfering RNA populations in wild-type and mutant flies. J. Virol. **85**(24), 13153–13163 (2011)
57. M.O. Delgadillo, P. Sáenz, B. Salvador, J.A. García, C. Simon-Mateo, Human influenza enhances viral protein NS1 virus pathogenicity and acts as an RNA silencing suppressor in plants. J Gen. Virol. **85**(Pt 4), 993–999 (2004)
58. C.M. Olsen, T. Markussen, B. Thiede, E. Rimstad, Infectious salmon anaemia virus (ISAV) RNA binding protein encoded by segment 8 ORF2 and its interaction with ISAV and intracellular proteins. Viruses. **8**(2), 52 (2016). https://doi.org/10.3390/v8020052
59. H. Yuwen, J.H. Cox, J.W. Yewdell, J.R. Bennink, B. Moss, Nuclear localization of a double-stranded RNA-binding protein encoded by the vaccinia virus E3L gene. Virology. **195**(2), 732–744 (1993)
60. J.M. Vargason, G. Szittya, J. Burgyán, T.M. Hall, Size selective recognition of siRNA by an RNA silencing suppressor. Cell **115**(7), 799–811 (2003)
61. K. Ye, L. Malinina, D.J. Patel, Recognition of small interfering RNA by a viral suppressor of *RNA silencing*. Nature. **426**(6968), 874–878 (2003)
62. H. Wang, L. Chang, X. Wang, A. Su, C. Feng, Y. Fu, D. Chen, N. Zheng, Z. Wu, MOV10 interacts with Enterovirus 71 genomic 5′UTR and modulates viral replication. Biochem. Biophys. Res. Commun. **479**(3), 571–577 (2016). https://doi.org/10.1016/j.bbrc.2016.09.112